ORIGINAL ARTICLE

Diversification and cryptic diversity of *Ophisops elegans* (Sauria, Lacertidae)

Claudine Montgelard[1,2] (iD) | Roozbeh Behrooz[1] | Véronique Arnal[1] | Atefeh Asadi[1] | Philippe Geniez[1] | Mohammad Kaboli[3]

[1]CEFE, PSL-EPHE (Biogéographie et Ecologie des Vertébrés), CNRS, Université de Montpellier, Univ Paul Valéry Montpellier 3, IRD, Montpellier, France

[2]Department of Zoology, Centre for Ecological Genomics and Wildlife Conservation, University of Johannesburg, Johannesburg, South Africa

[3]Department of Environmental Science, Faculty of Natural Resources, University of Tehran, Karaj, Iran

Correspondence
Claudine Montgelard, Biogéographie et Ecologie des Vertébrés (EPHE), Centre d'Ecologie Fonctionnelle et Evolutive (UMR 5175 CNRS), 1919 route de Mende, 34293 Montpellier cedex 5, France.
Email: claudine.montgelard@cefe.cnrs.fr

Abstract

Revealing cryptic diversity constitutes the backbone of the future identification and description of a new lineage. For the genus *Ophisops* (Lacertidae), previous studies indicated that this genus is characterized by cryptic diversity as three clades were obtained for *O. elegans* and *O. occidentalis* that do not fit the classical systematics. Notably, we were interested to delineate the distribution range of the two clades of *O. elegans* described in Iran. We sequenced 65 individuals of *Ophisops* mainly from northwestern Iran for one mitochondrial (*cytochrome c oxidase subunit 1* [*COI*]; 686 base pairs [bp]) and three nuclear genes (*R35*, *MC1R*, and *PKM2*; 1,857 bp). Phylogeographic analysis from mitochondrial and nuclear genes confirmed that Iranian samples belong to two major haplogroups (divergence of 13% for *COI*) that are also split into several subclades (divergence of 6%–10% for *COI*), revealing an unsuspected diversity within Iranian *Ophisops*. Divergence dating and biogeographical analysis indicated that most clades arose through vicariance and dispersal processes during the Mio-Pliocene (between 7.2 and 1 Myr). However, a scenario of expansion/regression is also advocated for explaining the distribution and contact between three subclades in North Iran. We propose to recognize the three major clades as three potential candidate species. Moreover, we found some correspondence between several phylogenetic clades or subclades identified and six of the nine subspecies described for *O. elegans*. Both species and subspecies delimitation and identification would deserve additional investigations (including morphology, ecology, biogeography, and behavior) to fulfill the conditions of integrative taxonomy.

KEYWORDS
biogeographical scenario, candidate species, mitochondrial *COI*, nuclear genes, phylogeography

1 | INTRODUCTION

Evolutionary studies based on molecular markers often lead to the discovery of cryptic genetic diversity that is the identification of diverged lineages within a species that are apparently morphologically indistinguishable. Revealing cryptic diversity is important for the description and understanding of biodiversity but it is unclear how this genetic diversity translates into actual species (Jorger & Schrodl, 2013). On this basis, molecular studies are often accused to inflate the number of species or subspecies (Torstrom, Pangle, & Swanson, 2014; Zachos et al., 2013) but new and more powerful morphological tools (such as geometric morphometrics) can lead to similar effects (Zuniga-Reinoso & Benitez, 2015). Since a few years, however, the number of papers including "cryptic species or speciation" seems to decrease (see Struck et al., 2018), probably in link with the recommendation for delineating and characterizing new species on the basis of integrative taxonomy (Dayrat, 2005; Padial, Miralles, De la Riva, & Vences, 2010; Schlick-Steiner et al., 2010). This approach of species delimitation combines different sources of information issuing from complementary disciplines, such as morphology, ecology, biogeography, or behavior in addition to molecular data. However, revealing cryptic diversity is the first step that leads to the identification of specific lineages that will have to be subsequently considered, notably in ecology, taxonomy, and conservation studies. Pending further investigations, it is still possible to propose candidate species that will be confirmed or rejected but that nevertheless represent independent evolutionary units.

In Lacertidae, species systematics is rendered difficult by high morphological similarities, great intraspecific variability and homoplasic (convergent) characters (Arnold & Ovenden 2010). In this context, DNA-based studies often revealed cryptic diversity and numerous discrepancies between the genetic clades evidenced and current systematics at the specific or subspecific levels, such as among the genera *Acanthodactylus* (Tamar et al., 2016), *Eremias* (Guo et al., 2011), or *Mesalina* (Kapli et al., 2015) to quote only a few examples among Eremiadinae (Arnold, Arribas, & Carranza, 2007). Within this subfamily, the genus *Ophisops* conforms to this rule. Snake-eyed lizards (so named for the absence of mobile eyelid) are distributed from North Africa until South of India and Sri Lanka. Two disjoint biogeographical units (India and Saharo-Arabia) are recognized within which morphological taxonomy recognized eight species until recently (Agarwal & Ramakrishnan, 2017; Uetz, Freed, & Hošek, 2019). However, diversity among *Ophisops* is suspected to be largely underestimated in the Middle East (Kyriazi et al., 2008) or in India where the phylogenetic study of Agarwal and Ramakrishnan (2017) identified not <30 new candidate species. *Ophisops* is split into a small-bodied (snout to vent length, SVL < 45 mm) and a large-bodied (SVL > 50 mm) clade (Agarwal & Ramakrishnan, 2017) with the Saharo-Arabian species group (*O. elegans*, *O. occidentalis*, and *O. elbaensis* under classical taxonomy ; see Uetz et al., 2019) nested among the latter. However, diversity in this group is suspected to be underestimated as indicated by the molecular phylogenetic analysis of Kyriazi et al. (2008) which revealed three major clades (A, B, and C). The clade A is distributed from Greece to Jordan in the south (Cyprus included), the Republic of Azerbaijan in the north and western-central part of Iran. The group B is represented by individuals from Tunisia, Libya, and Israel, and all individuals attributed to *O. occidentalis* were included in this group (thus rending *O. elegans* polyphyletic). The group C is constituted of four individuals from north-east Turkey, Armenia and north-west Iran. At the subspecific level, the taxonomy of *O. elegans* is in even more turmoil. Indeed, nine subspecies have been described based on morphological characters and despite taxonomic revisions (Darevsky & Beutler, 1981; Disi, 2002; Lymberakis & Kaliontzopoulou, 2003; Moravec, 1998) phylogenetic relationships and subspecies identification of *O. elegans* are still uncertain.
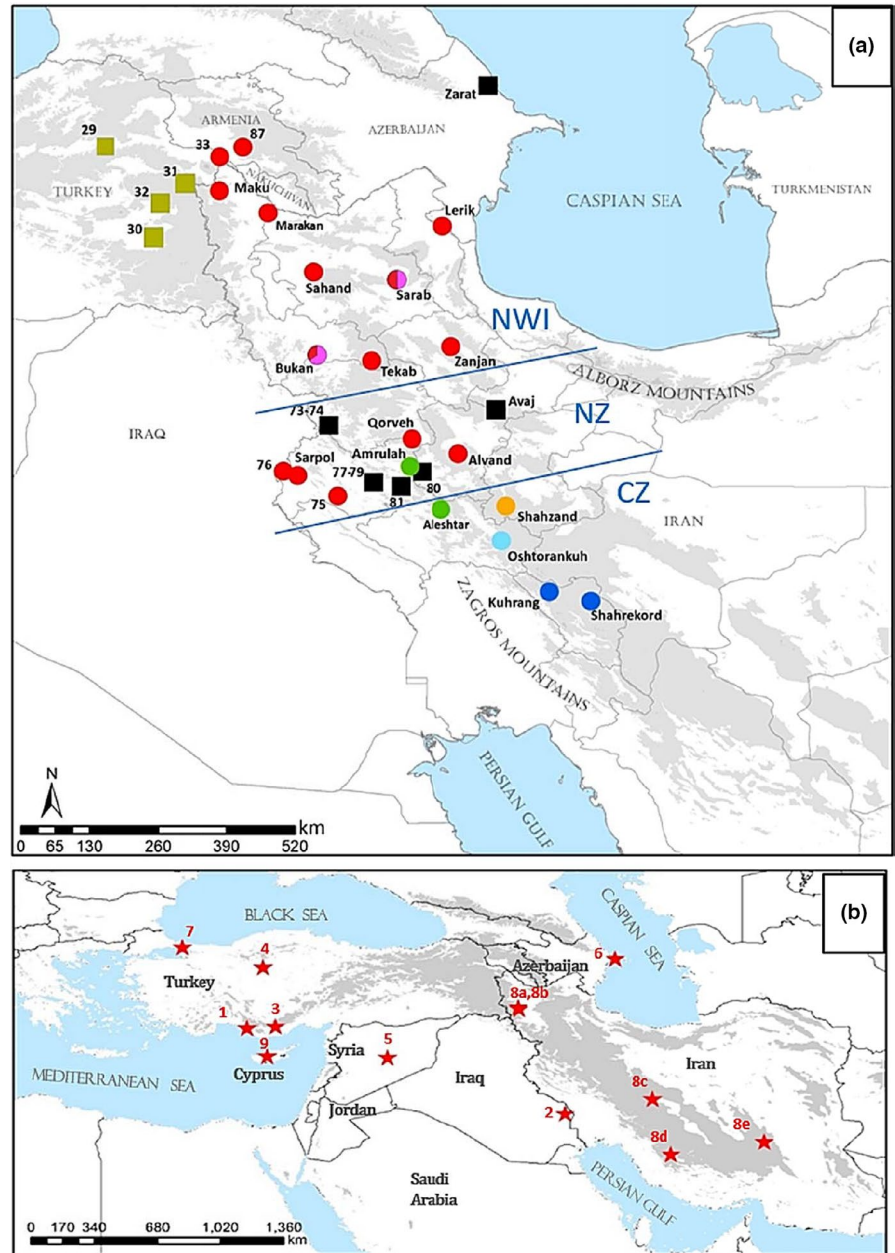
The aim of the present study was to further understand the evolutionary history of *O. elegans*, particularly in extending the sampling in Iran in order to better delineate the two Iranian clades presently described in the study of Kyriazi et al. (2008). By its geographic position, Iran is at the intersection between Palearctic (Western and Eastern) and Saharo-Arabian realms (Yusefi, Safi, & Brito, 2019), and thus, fauna is under the influence of both biogeographical regions. By its position, Iran makes the connection between Palearctic and Indian distribution of *Ophisops*, and thus, we could expect a better understanding of the diversification of the genus. Notably, two dispersal events have been evidenced into and out-of-India (Agarwal & Ramakrishnan, 2017) thus questioning the tempo and timing of the Saharo-Arabian diversification of *Ophisops*. In this context, our objectives were to answer the following questions: (a) what is the distribution range of both lineages observed in Iran and does more cryptic diversity can be uncovered? (b) What is the age of the different *O. elegans* clades: was the diversification of the *Ophisops* lineages mainly modeled by recent events (such as Quaternary glacial cycles) or by older events? (c) Can we propose a biogeographical scenario explaining the diversification of *O. elegans* in Iran? The objective will be here to evaluate the relative importance of vicariance and dispersal in shaping the phylogeographical pattern of *O. elegans*. Our study revealed important cryptic diversity within *O. elegans* that questioned the present taxonomy both at the specific and subspecific levels. In analyzing the level of correspondence between the species/subspecies described and the genetic clades (cryptic diversity) observed, we tentatively propose some taxonomic reassessments for *O. elegans*.

2 | MATERIAL AND METHODS

2.1 | Sampling and sequencing

Our sampling included 65 specimens from 17 localities in Iran, two in Azerbaijan, and one in Turkey (see Figure 1a and Appendix 1). Iranian tissue samples (a small piece of tail) were obtained from individuals captured during fieldwork conducted under the permission

FIGURE 1 (a) Distribution of our sampling of *Ophisops elegans* (see also Appendix 1) with the different colors corresponding to the different clades observed (see Figure 2 and Figure S1). Localities from clade A and C are represented by square and circle, respectively. Numbers correspond to the code locality for specimens studied by Kyriazi et al. (2008, appendix A). NWI, NZ, and CZ, respectively, represent the North-West Iran, North Zagros, and Central Zagros areas as used in the BioGeoBears analysis. (b) Type localities for the nine subspecies described for *O. elegans*: 1—*O. e. basoglui*, 2—*O. e. blanfordi*, 3—*O. e. budakibarani*, 4—*O. e. centralanatoliae*, 5—*O. e. ehrenbergii*, 6—*O. e. elegans*, 7—*O. e. macrodactylus*, 8—*O. e. persicus*, and 9—*O. e. schlueteri* (see Table S3 for references)

(98/400/4493) of the Iranian Department of Environment. Other samples were supplied from the Biogéographie et Ecologie des Vertébrés collection hosted in the Centre d'Ecologie Fonctionnelle et Evolutive in Montpellier, France. Three different species of *Eremias* (*E. velox*, *E. arguta*, and *E. persica*) have been used as outgroups (see Appendix 1).

Total genomic DNA was extracted from tissue samples using the Qiagen DNeasy Tissue kit, following the manufacturer's instructions (Qiagen). We sequenced a fragment of the mitochondrial *cytochrome c oxidase subunit 1* (*COI*; PCR product of 737 bp) for 65 *O. elegans* as well as three fragments of nuclear genes for 20 *O. elegans* and the three *Eremias* species (see Appendix 1): partial intron of the *RNA fingerprint protein 35* gene (*R35*; PCR product of 749 bp), partial sequence of the *melanocortin receptor 1* gene (*MC1R*; PCR product of 749bp), and partial intron 5 of the *muscle pyruvate kinase* gene (*PKM2*; PCR product of 528bp). All fragments were amplified through polymerase chain reaction (PCR) using primers and conditions given in Table S1.

All PCR products were sent to Eurofins Genomics for sequencing. Chromatograms were read and aligned using CodonCode Aligner 4.2.5 (LI-COR, Inc.). Forward and reverse sequences were checked by eye, and a consensus sequence was compiled with CodonCode Aligner. All *COI* sequences have been translated into amino acids to check for possible amplification of pseudogenes. A total of 65 *COI* and 66 nuclear sequences have been deposited at the National Center for Biotechnology Information (see Appendix 1 for accession numbers). Our dataset was completed in including 93 *COI* sequences (398–470 bp) downloaded from NCBI (accession numbers EU081519–EU081610 from Kyriazi et al., 2008 and AF206556 from Fu, 2000). All sequences were aligned using ClustalW as implemented in Bioedit 7.2.5 (Hall, 1999).

2.2 | Phylogenetic reconstructions

Phylogenetic trees were reconstructed using two probabilistic methods: maximum likelihood (ML) with RaxML8.0 (Stamatakis, 2014) and Bayesian inference (BI) with MrBayes3.2 (Ronquist & Huelsenbeck, 2003). The best partitioning scheme and model of sequence evolution were inferred for both methods with PartitionFinder (Lanfear, Calcott, Ho, & Guindon, 2012) using the greedy algorithm and the Bayesian information criteria for four different datasets (see Table S2). MrBayes was run for 10 million generations sampled every 500th generation and a burn-in of 2,000 (trees and parameters). RaxML was run using the model GTR + G applied to each partition specified with PartitionFinder. Nodal support was evaluated with 1,000 bootstrap replications, and the extended majority rule consensus tree was calculated with RaxML (command –J MRE).

2.3 | Divergence dating

Estimations of node age (or divergence times) were performed with Beast v1.10.4 (Suchard et al., 2018) and calculated using three calibrations points (see Psonis et al., 2018): (a) the divergence of *Lacerta viridis* with respect to other *Lacerta* species using a normal prior distribution (8.70 ± 0.5 Myr; Venczel, 2006); (b) the divergence between *Podarcis peloponnesiacus* and *P. cretensis* arising from the isolation of Crete from Peloponnesus at 5.3 ± 0.5 Myr (Poulakakis et al., 2005); and (c) the split between *Podarcis lilfordi* and *P. pityusensis* resulting from the separation between different Balearic islands (Mallorca, Menorca, Cabrera vs. Ibiza, Formentera, respectively; Terrasa, Picornell, Castro, & Ramon, 2004) and dated at 5.25 ± 0.03 Myr (Brown et al., 2008). All six species mentioned above were added to our dataset (see Appendix 1 for *COI* accession numbers) represented by one sequence for each *Ophisops* candidate species (as determined with BPP).

Three molecular clock models were tested (strict clock, lognormal, and exponential uncorrelated relaxed clock) using a Yule speciation process as tree prior for each clock model. The three molecular dating analyses were run using the model TrN + G (as determined with PartitionFinder) applied to each codon position with unlinked parameters across codon position. Beast was run for 50 million generations sampled every 5,000th. The best molecular clock model was selected based on the Akaike's information criterion through Markov chain Monte Carlo (AICM) as calculated with Tracerv1.6 (Rambaut, Drummond, & Suchard, 2013) using 100 bootstrap replicates. The maximum clade credibility (MCC) tree was obtained with TreeAnnotator in Beast after a 10% burn-in (1,000 trees).

2.4 | Genetic diversity, network, and demographic analyses

Several molecular diversity indices were calculated using DNAsp v5 (Librado & Rozas, 2009): the number of haplotypes (*h*), the number of polymorphic sites (*S*), the haplotype (Hd) and nucleotide (pi) diversities, and the average number of nucleotide differences (*k*). The haplotype network was built using the TCS option in PopART (Leigh & Bryant, 2015), and the intra- and inter-group genetic divergence using the *p*-distance was calculated with MEGA6 (Tamura, Stecher, Peterson, Filipski, & Kumar, 2013).

Demographic inferences of Ne (effective population size) in the course of time were assessed with Beast v1.10.4 using the Bayesian skyline as coalescent. For each demographic analysis, the nucleotide substitution model GTR + G was applied to each *COI* codon position (three partitions with unlink parameters) and a strict molecular clock was applied using as prior the mean rate obtained in the divergence dating analysis (see section 3). Beast was run for 50 million of generations sampled every 1,000th, and Bayesian skyline plots (BSP) were calculated with Tracer after a 10% burn-in.

2.5 | Historical biogeography

Several biogeographical models of ancestral-range estimation were tested with the R package BioGeoBEARS (Matzke, 2013) for the clades A and C of *O. elegans* (see Figure S1). We used the chronogram previously obtained from the divergence dating analysis (Figure 4) that was pruned using the software Mesquite 3.6 (Maddison & Maddison, 2018) to remove the six outgroups and *Ophisops jerdonii*.

Seven main geographical areas have been defined among the distribution area of *O. elegans*: North-West Iran (NWI, clade C1–C2), Central Zagros (CZ, clade C3–C6), North Zagros (NZ, clade A4 of Kyriazi et al., 2008), West Turkey (WT clade A1), South-East Turkey-Syria-Lebanon-Jordan (JS, clade A2), Centre to East Turkey (ET, clade A3), Cyprus (Cy, clade A5). Three models have been evaluated: the dispersal–extinction–cladogenesis (DEC), the dispersal–vicariance (DIVALIKE), and the Bayesian inference of historical biogeography for discrete areas (BAYAREA). Each model was analyzed with and without the parameter J representing the founder-event speciation (rare long-distance dispersal event), thus representing a total of six models tested. BioGeoBEARS was run with the option unconstrained meaning that there was no constrain on the dispersal directionality since the three ancestral areas.

2.6 | Species delimitation

Joint Bayesian species delimitation and species tree estimation (analysis A11, unguided species delimitation) was conducted using the program BPP3.4a (Yang, 2015). Analyses were conducted using the rjMCMC (1 1 2 1) algorithm whereas default priors/values were used for other parameters (thetaprior, tauprior, finetune). The MCMC chain was run for 200,000 generations with a burn-in of 15,000, and each analysis was run twice to check for consistency.
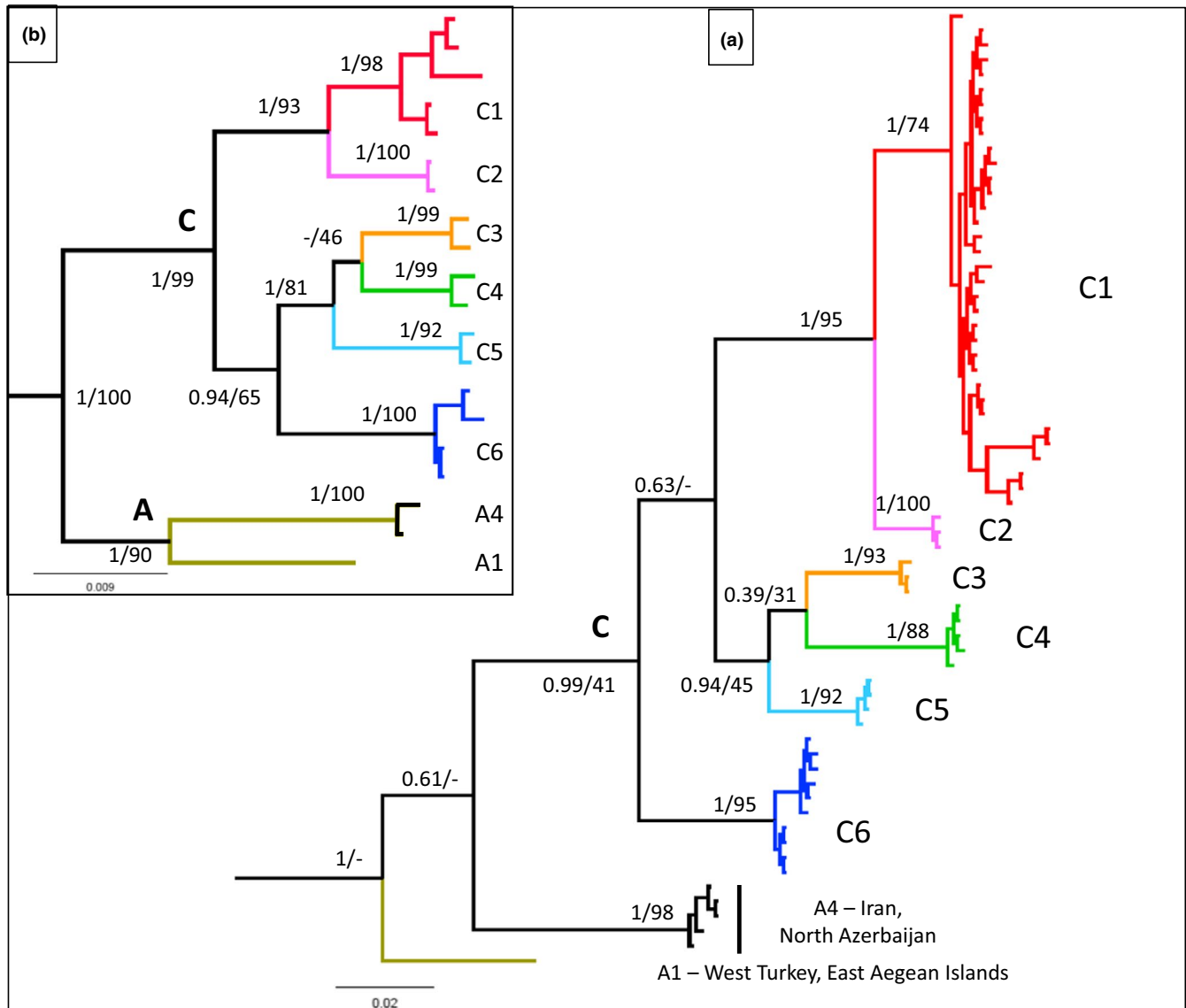
FIGURE 2 Bayesian phylogenetic trees of (a) the *COI* sequences (65 samples, 686 positions) and (b) the concatenated *COI* and nuclear genes (20 sequences, 2,543 positions). In both cases, phylogenetic trees were rooted using three *Eremias* species (not shown) and numbers at nodes refers to posterior probabilities obtained with MrBayes and bootstrap proportions obtained with RaxML after 1,000 replicates, from left to right, respectively. The color code is the same as in Figure 1

3 | RESULTS

3.1 | Phylogenetic analysis

A first analysis was performed with the 65 *COI Ophisops* sequences (final alignment including 686 bp; 171 variable positions; see Alignment S1) obtained in this study (see Table S2 for best partitions and models). The phylogenetic tree (Figure 2a) revealed that most individuals are grouped in one clade corresponding to the clade C of Kyriazi et al. (2008). This grouping included six well-supported phylogroups (C1–C6 represented by different colors in Figures 1 and 2) that are mostly consistent with geographical localities. C1 included populations from north of Iran (Maku, Marakan, Sahand, Sarab, Bukan, Tekab, Zanjan, Sarpol-e-Zahab, Qorveh, and Alvand) as well as one locality from south-eastern

Azerbaijan (Lerik). The clade C2 included individuals from Sarab and Bukan. The populations from Shazand and Oshtorankuh formed the groups C3 and C5, respectively, whereas the group C4 included individuals from Aleshtar and Amrulah. Finally, populations of Kuhrang and Shahrekord constituted the phylogroup C6. Thus, only the two localities of Sarab and Bukan are distributed in more than one clade (C1 and C2) whereas only six individuals did not belong to the clade C (see below). The cluster C1–C2 is well supported, whereas no relationship is clearly supported among C3–C6.

A second analysis was performed on 158 *COI* sequences (our 65 samples + 93 sequences from GenBank) representing three *Ophisops* species (152 *O. elegans*, five *O. occidentalis* and one *O. jerdonii*) from 12 countries (Greece, Turkey, Syria, Jordan, Lebanon, Israel, Cyprus, Iran, Libya, Armenia, Tunisia, and India). The resulting phylogenetic tree (Figure S1) allowed replacing our samples in the framework of the
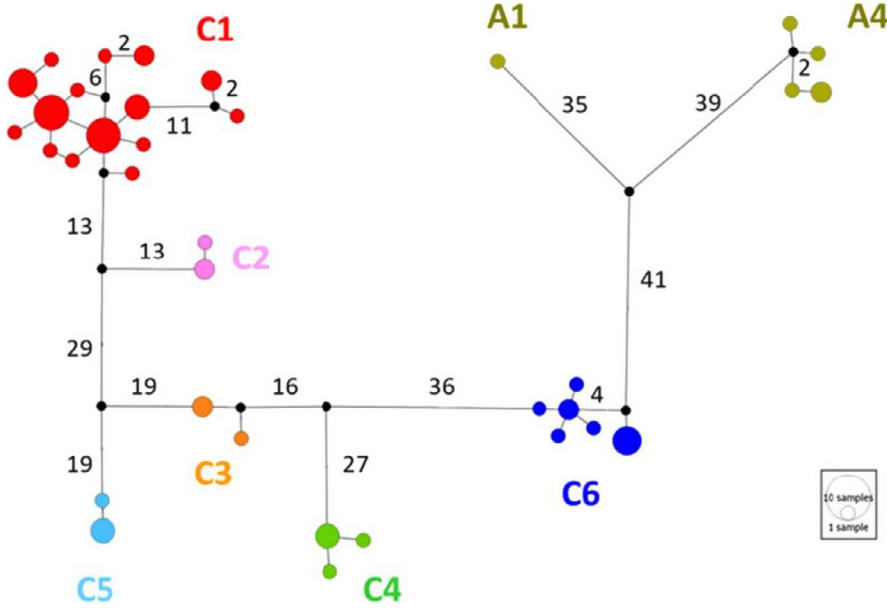
FIGURE 3 Haplotype network built with 64 *COI* sequences (686 positions). The size of each circle is proportional to the haplotype frequency, and the number of inferred substitution is noted on lines when different from 1. Clade name and code color are the same as in Figure 1

different clades identified by Kyriazi et al. (2008). Thus, all of our samples fell in their clade C with the exception of six individuals among them one is included in clade A1 (Turkey: Akseki) and five in clade A4 (two from Iran: Avaj and three from Azerbaijan: Zarat). The four individuals from Turkey (33, Aralik in Figure 2), Armenia (87, Chosrov), and Iran (75, Eslamabad and 76, Ghasr-e-shirin) that represented the clade C in Kyriazi et al. (2008) are all included in our phylogroup C1 (see Figure 1). As expected, no sample from our study fell in the clade B which represents individuals from North Africa and Israel. If the monophyly of the three major clades appeared moderately (B and C) or not (A) supported, all subclades are very well supported although relationships between them are not resolved, particularly among clade A and C3–C6 (Figure S1).

The final alignment of the three nuclear genes represented 1,857 positions (see Alignment S2): 690 for *R35* (23 variable positions), 692 for *MC1R* (14 variable positions), and 475 for *PKM2* (29 variable positions) for 20 *Ophisops* specimens belonging to the different phylogroups obtained with *COI* and the three *Eremias* species as outgroups (see partitions and models in Table S2). The phylogenetic tree (data not shown) indicates that the monophyly of phylogroups A and C is robustly supported whereas among clade C only the subclades C1, C2, C5, and C6 are strongly to moderately supported.

Finally, *COI* and the three nuclear genes were combined for 20 *Ophisops*, thus representing 2,543 aligned positions (see Table S2 for the best partitioning and models). The phylogenetic tree (Figure 2b) allowed recovering all clades identified with the *COI* but with a stronger support, notably the monophyly of phylogroups A and C is now well supported as well as three groupings among clade C (C1–C2, C3–C6, and C3–C5).

3.2 | Network, genetic diversity, and historical demography

The network (Figure 3) was constructed on 686 positions of the *COI* for 64 *Ophisops* (one individual NEZMUT1765 from Tekab

was removed because of a shorter sequence) and allowed to recover all groups obtained in the phylogenetic tree. The two major phylogroups (A and C) are separated by a high number of positions (41). Among each of the two major groups, the subclades identified are also distantly separated by a comparable number of positions whereas the variability among each clade appeared more limited. The haplotype diversity is high whatever the group or subgroups considered (Table 1) but the nucleotide diversity is rather low, particularly within subclades (C1 or C6).
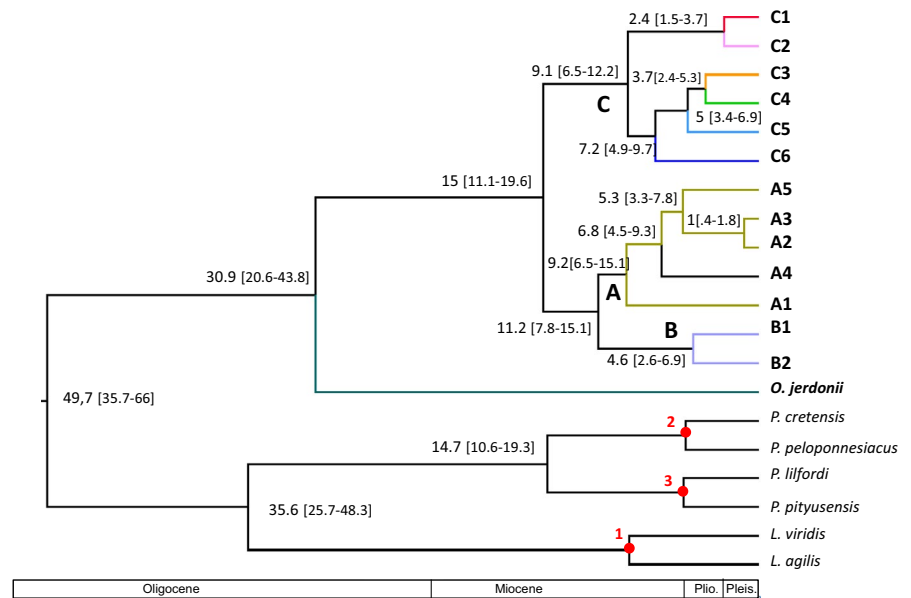
For *COI*, the genetic divergence, as measured with the *p*-distance (Table 2), indicated that the intra-clade divergence reach about 6% for clades C and C3–C6 whereas the inter-clade distances are above 10% including between the two major C groups (C1–C2 vs. C3–C6). The same pattern is obtained with the nuclear dataset although the *p*-distances are much lower (1.5% as inter-clade distances).

Demographic inferences were performed with Beast on clades C1–C2 (36 individuals), C3–C6 (22 individuals), and A4 (12 individuals) using the mean substitution rate (0.0106 substitution per site per Myr) obtained from the divergence dating analysis (see below). The BSP diagrams (Figure 5) indicated that the two first groups (C1–C2 and C3–C6) showed a recent expansion (about 90 and 50 Kyr ago, respectively) after a more ancient period of decline (about 250 and 500 Kyr ago). By contrast, the A4 group is currently in phase of stagnation/decline since about 20 Kyr after a period of expansion (140–160 Kyr ago). It can be noted that if the general pattern is the same for the two C groups, the timings of decline/expansion are not synchronous.

3.3 | Species delimitation

The first BPP analysis was run on a dataset of 65 *Ophisops COI* (clades A, B, and C), thus representing eight "potential species" (A1, A4, C1, C2, C3, C4, C5, and C6; see Figure 1). This analysis gave support for a delimitation model in eight "species" with a posterior probability of 1.

FIGURE 4 *Ophisops* Beast chronogram of the *COI* sequences. Numbers at node refer to the divergence time in Myr with 95% HPD into brackets. The three red points correspond to the three calibration points used: 1, the divergence between *Lacerta agilis* and *Lacerta viridis* calibrated at 8.70 ± 0.5 Myr; 2, the divergence between *Podarcis cretensis* and *P. peloponnesiacus* at 5.3 ± 0.5 Myr; 3, the divergence of *Podarcis lilfordi* and *P. pityusensis* at 5.25 + 0.03 Myr. Code color for clades is the same as in Figures 1 and 2

A second analysis was performed on the whole *COI* dataset including 120 *Ophisops* representing 13 *Ophisops* clades (A1, A2, A3, A4, A5, B1, B2, C1, C2, C3, C4, C5, and C6; see Figure S1). In this case also, thirteen "species" were identified with a posterior probability of 1 for each run. Finally, a BPP analysis was conducted on the nuclear dataset only (20 *Ophisops* from clusters A1, A4, C1, C2, C3, C4, C5, and C6; see Figure 1). In this case, the analysis returned a posterior probability of 0.7 for six distinct "species" (C1C3C4, C2, C5, C6, A4, and A1) and 0.3 for seven "species" (C1, C2, C3C4, C5, C6, A4, and A1).

3.4 | Divergence dating

Divergence times were calculated on the most complete *COI* dataset in taking only one sequence for each of the 13 potential candidate species determined with BPP (i.e., five, two, and six for clades A, B, and C, respectively) and *O. jerdonii*. All the three Beast analyses performed with three clock models converged with significant ESS values (>500) for all parameters. The model comparison analysis performed with TRACER identified the strict clock as the best

molecular clock model as compared to the exponential and lognormal relaxed clocks (ΔAICM = 202.3 and 207.0, respectively). The MCC tree (Figure 4) indicated that the split between *O. jerdonii* and *O. elegans* + *O. occidentalis* is dated at 30.9 Myr (95% HPD: 20.6–43.8). The two main clades (A and C) originated at 11.2 (95% HPD: 7.8–15.1) and 9.1 Myr (95% HPD: 6.5–12.2), respectively, whereas the origin of clade B is dated at 4.6 Myr (95% HPD: 2.6–6.9). Among clades A and C, the successive splits (clades C1–C6 and A1–A5) are distributed between 9.2 and 1 Myr (see Figure 4 for 95% HPD).

3.5 | Biogeographical scenario

On the basis of the AIC criterion, it can be noted that the inclusion of the parameter J (founder-event speciation) significantly improved the log-likelihood for each of the three model tested (Table 3). BioGeoBEARS identified DEC + J and Divalike + J (showing nearly the same AIC value) as the best biogeographical models explaining the distribution pattern of *O. elegans*. Thus, BioGeoBears favored both a scenario of vicariance, (notably in clade C; see Figure S2) and dispersal. Both models also

TABLE 1 Genetic diversity indices for different haplogroups evidenced with the *COI* dataset

Phylogroup	N	h	S	Hd ± SD	Pi ± SD	k
TOTAL	64	34	162	0.97 ± 0.01	0.074 ± 0.006	47.53
Clade C	58	29	125	0.96 ± 0.01	0.061 ± 0.005	39.39
Subclade C1–C2	36	16	47	0.91 ± 0.03	0.013 ± 0.003	8.57
Subclade C1	33	14	36	0.90 ± 0.03	0.007 ± 0.002	4.80
Subclade C3–C6	22	13	95	0.94 ± 0.03	0.059 ± 0.004	40.80
Subclade C6	10	6	9	0.84 ± 0.10	0.005 ± 0.001	3.47
Clade A	6	5	79	0.93 ± 0.12	0.040 ± 0.023	27.20

Abbreviations: *h*: number of haplotype; Hd: haplotype diversity; *k*: average number of nucleotide differences; *N*, number of individuals; Pi: nucleotide diversity; *S*: number of polymorphic sites; *SD*: standard deviation.

TABLE 2 Percentage of divergence (*p*-distance) between the main phylogroups evidenced using the mitochondrial (*cytochrome c oxidase subunit 1*) and nuclear (three genes) datasets, below and above the diagonal, respectively

	Clade C	C1–C2	C3–C6	Clade A
Clade C	6.0/0.44	—	—	1.5 ± 0.26
C1–C2	—	1.3/0.42	0.52 + 0.09	1.5 ± 0.27
C3–C6	—	9.9 ± 0.9	6.0/0.32	1.5 ± 0.26
Clade A	13.0 + 1.0	14.1 ± 1.2	12.4 ± 1.1	4.0/0.53

Note: On the diagonal is given the intragroup percent of divergence (*p*-distance) for the mitochondrial/nuclear datasets, respectively.

include the parameter J (founder-event speciation) to take into account rare long-distance dispersal events, such as between clades found in North Zagros (A4, C1–C2, and C4; see Figure 1).

4 | DISCUSSION

4.1 | Diversification of *Ophisops* in the Middle East

In the context of the three main clades (A, B, and C) retrieved for *O. elegans* + *O. occidentalis* by Kyriazi et al. (2008), our study allowed

completing the distribution area for the clade C, notably with 17 new localities in Western Iran and two in the Republic of Azerbaijan. The noteworthy fact is that each of these three major clades is highly structured (see Figure S1) as five subclades were recognized for the clade A and two groups were identified for clade B by Kyriazi et al. (2008). Concerning the clade C, six groups were recovered in the present study among which two major clades can be recognized (see below). This pattern is revealed not only with the mitochondrial genes but also with the nuclear genes (Figure 2b) even though the genetic differentiation is much lower in this case (Table 2). Such cryptic diversity is not restricted to the Saharo-Arabian species group of *Ophisops* as shown by the study of Agarwal and Ramakrishnan (2017) performed on Indian *Ophisops*. These authors recognized about 30 candidate species (as compared to the five species traditionally recognized in India), among which two were recently described in the *Ophisops microlepis* complex (Agarwal, Khandekar, Ramakrishnan, Vyas, & Giri, 2018).

The study of Agarwal and Ramakrishnan (2017) clearly shown that the Saharo-Arabian clade (including *O. elegans* and *O. occidentalis*) is nested within the Indian large-bodied clade of *Ophisops*, thus suggesting a western dispersal from India. The biogeographical analysis performed with BioGeoBEARS revealed that both vicariance and dispersal events can explain the phylogeographical pattern observed for clades
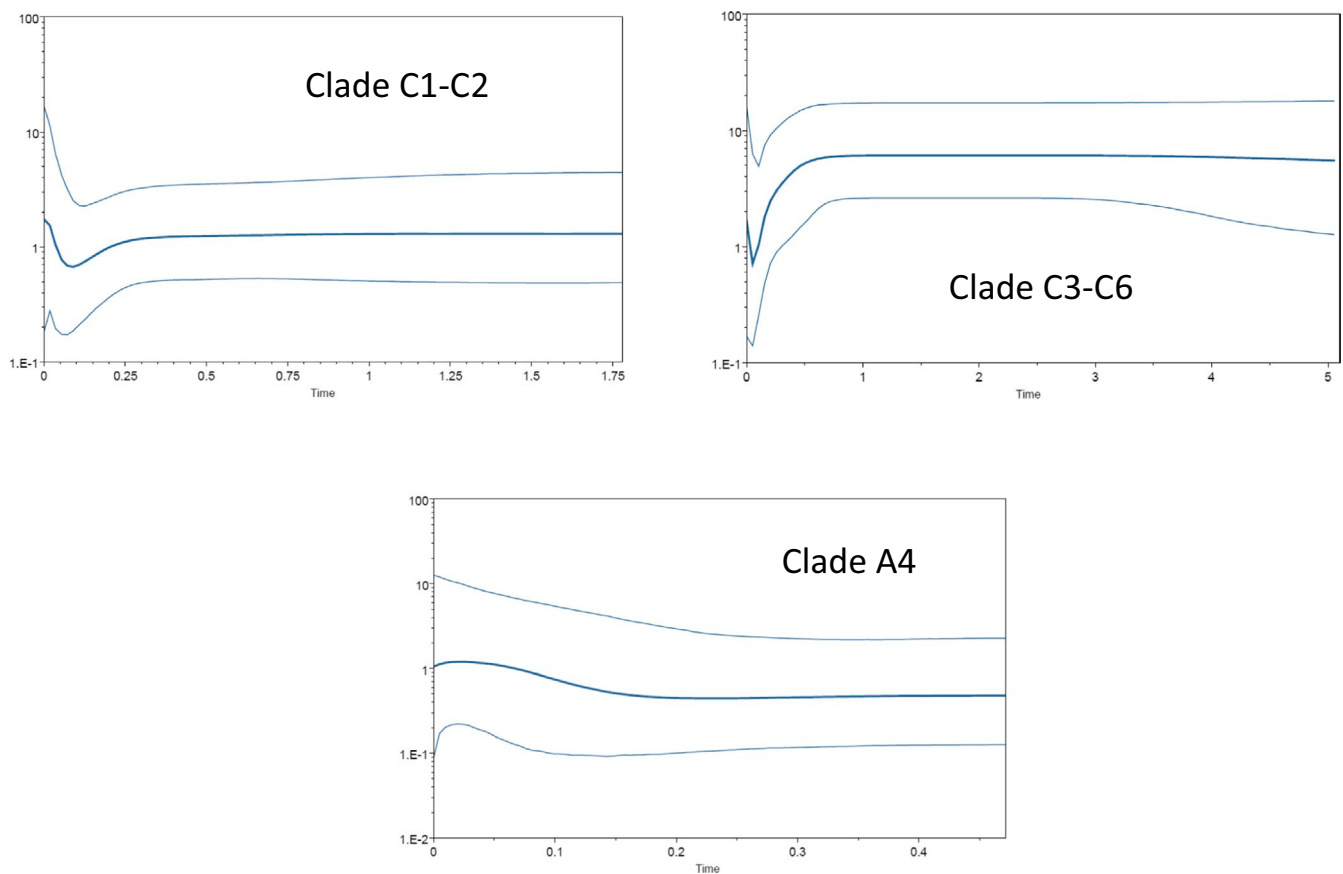

FIGURE 5 Bayesian Skyline Plots performed with Beast on three clades of interest. Time (expressed in Myr) and effective population size are reported on the *x*- and *y*-axes, respectively. Time was calculated using the mean substitution rate (0.0106 substitution per site per Myr) obtained in the divergence dating analysis. The two gray lines show the 95% highest posterior density of the median estimate (dark blue line)

TABLE 3 BioGeoBears analysis for six models of ancestral-range estimations: loglikelihoods (LnL), Akaike information criteria (AIC), and estimated parameters: rate of dispersal (*d*), rate of extinction (*e*) and founder-event speciation (*J*)

Model	LnL	AIC	*d*	*e*	*J*
DEC	−31.19	66.38	0.030	0.03	0
DEC + J	**−26.51**	**59.02**	**0.008**	**0**	**0.146**
DIVALIKE	−28.11	60.23	0.023	0	0
DIVALIKE + J	**−26.54**	**59.08**	**0.012**	**0**	**0.060**
BAYAREA	−32.26	68.52	0.033	0.05	0
BAYAREA + J	−27.38	60.77	0.048	0.01	0.081

Note: In bold are represented the best models according to the lowest AIC value.

Abbreviations: BAYAREALIKE, Bayesian inference; DEC, dispersal–extinction–cladogenesis; DIVALIKE, dispersal–vicariance analysis.

A and C of *O. elegans* in the Middle East. Vicariant events are suggested for clade C (from north-west Iran for clade C1–C2 and central Zagros for clade C3–C6; Figure S2) whereas diversification of clade A would be better explained by dispersal events (possibly from west to east Turkey and Iran). It is however difficult to infer the geographic origin of group A because of the lack of resolution among the A1–A5 clades.

Our divergence estimations (Figure 4) indicated that *O. jerdonii* diverged from *O. elegans* + *O. occidentalis* (Clades A + C) about 31 Myr ago (95%HPD: 20.6–43.8) in the Oligocene, a divergence time which is totally in agreement with the date of 30 Myr obtained by Agarwal and Ramakrishnan (2017) and much older than the 8.11 Myr of Kyriazi et al. (2008). The origin of clades A and C is dated at 9.1 (6.5–12.2) Myr which is slightly older but compatible with the estimations of 7.5 Myr obtained by Kyriazi et al. (2008) for clade A. Among the clades A and C, the splits into the different subclades spread from 7.2 to 1 Myr, that is over a period of several millions of years over the Upper Miocene and the Pliocene. Clearly, the diversification pattern of *Ophisops* does not result from recent events (such as Quaternary cycles) but rather could be traced back to the late Miocene (11.6–5.3 Myr). As also advocated by Agarwal and Ramakrishnan (2017) for Indian *Ophisops*, this diversification might be related to the expansion of open habitats (in which *Ophisops* is found) that followed aridification periods that occurred in the Middle East during the Upper Miocene (Ballato et al., 2010; Fortelius et al., 2006; Tang & Ding, 2013). The Plio-Pleistocene (last ~ 5 Myr) which is characterized by successive punctuations of cooler, drier, and more open conditions linked to the expansion of ice sheets at high-latitude (from 3.2 to 1 Myr; DeMenocal, 2004; Webb & Bartlein, 1992) might have led to different phases of expansion/contraction in the Saharo-Arabian *Ophisops*. However, a more comprehensive scenario explaining the diversification of Saharo-Arabian *Ophisops* would necessitate the inclusion of specimens from Southern Iran, Afghanistan, and Pakistan. Moreover, the taxonomic status and interactions of *O. elegans* and *O. occidentalis* would also deserve additional sampling notably from North Africa to Israel.

4.2 | Phylogeography at the Iran scale

Two main phylogeographic groups are observed in Iran, namely clades A and C but their distribution appears quite different. Subclade A4 is found in northern Zagros in the western part of Iran (black squares in Figure 1) whereas clade C is found from East Turkey and Armenia in the North to the central Zagros in Iran. The two major subclades observed are geographically juxtaposed with C1–C2 occupying the north-west of Iran and C3–C6 the central Zagros in western Iran. The genetic structure of the two subclades appeared also different. C1–C2 showed little structure especially the group C1 which includes numerous individuals (33 samples from 11 localities) but shallow differentiation (14 haplotypes but weak nucleotide diversity; see Table 1). The population mixing between C1 and C2 observed in Bukan and Sarab localities might be the result of dispersal events from clade C1 to C2 (see below). By contrast, the clade C3–C6 appeared genetically and geographically highly structured. These three groups (C1–C2, C3–C6, and A4) come into contact in the central part of the Zagros (from Ghasr-e-shirin close to the Irako–Iranian border to Avaj in the Qazvin province; Figure 1).

Thus, it can be concluded that the *Ophisops* diversity revealed in Iran was hitherto unsuspected and clearly represents cryptic diversity (no difference in coloration pattern or external morphology was observed). The genetic divergence between the two main groups observed in clade C (about 10%) mainly distributed in Iran is comparable to the genetic distances detected for *COI* between the five subclades A distributed from Greece to Azerbaijan and Jordan (10.3%; Kyriazi et al., 2008). Moreover, several subclades are observed in Iran but this diversity might still be more important as it is clear that the geographical distribution of the two main subclades is not definitely settled, particularly in the eastern and southern parts of Iran where *O. elegans* was recently found (Oraie, Rahimian, Rastegar-Pouyani, Rastegar-Pouyani, & Khosravani, 2012).

We have seen previously that the historical biogeography analysis (Figure S2) suggested a scenario of vicariance for explaining the distribution of the different groups evidenced in the clade C. However, in this context the North Zagros does not fit very well to this hypothesis as haplotypes in this region fall in several clades: A4, C1–C2, C3–C6 without speaking of the locality of Zarat (Azerbaijan) close to the Caspian sea which appears isolated from other members of the subclade A4 (Figure 1). The question is how to explain such a striking pattern. The demographic analyses (Figure 5) indicated an expansion pattern for the clades C1–C2 and C3–C6 but a decreasing curve for the clade A4. Thus, it might be hypothesized that, as a consequence of range expansion, the C clades (especially C1) are in the course to replace and eliminate the subclade A4 (and probably C2 as well), thus currently living only the north (Azerbaijan) and the western-central Iran to A4. It seems also that the C3–C6 clade is progressing from South to North of Iran as the most ancestral group (C6) is located in the south and the most recent (C3–C4) in the north (see Figures 1 and 2b). However, as each subclade is represented by a few individuals

(particularly A4), more sampling in key (but difficult to access) regions such as Iraq, Syria as well as Armenia and Azerbaijan would be necessary to give support to this scenario.

4.3 | Taxonomic consideration

As stated previously, cryptic diversity appeared to be the rule rather than the exception among different *Ophisops* species (Kyriazi et al., 2008; Agarwal & Ramakrishnan, 2017; present study). For *O. elegans* and *O. occidentalis*, three main clades (A, B, and C) were observed that do not match with the current systematics as *O. occidentalis* is nested among the clade B of *O. elegans* (Kyriazi et al., 2008). Moreover, the percent of uncorrected-divergence between the three major clades amounts to 13% with respect to *COI* sequences. Even if the divergence is much lower when nuclear genes are compared (1.5%), the same phylogroups are recovered (at least for clades A and C). Such cryptic diversity points to the need for a taxonomic re-evaluation, notably at the species level. In this context, we can propose the clades A, B, and C as potential candidate species and we can tentatively advance a species name for these three clades. Clade A could tally with *O. elegans* as the type locality (Baku, Azerbaijan; Ménétries 1832) fall in the clade A4 (see Figure S1). Clade B could correspond to *O. occidentalis* which was originally described from Algeria and Tunisia (Boulenger, 1887), the latter being included in clade B2 (see Figure S1). As the clade C is mainly distributed in Iran, the subspecies *Ophisops elegans persicus* (described from several localities from Iran; see below) might be elevated to the species rank (*O. persicus*). Of course, these propositions would deserve additional investigations (including morphology, ecology, and distribution) to fulfill the conditions of integrative taxonomy. Settling the issue would also necessitate getting a better delineation of the distribution area for some clades (notably B and C) as well as including some specimens of *O. elbaensis*. Indeed, no sequence is available for this species (distributed in the Near and Middle East; Uetz et al., 2019) which is also a member of the Saharo-Arabian species group of *Ophisops*.

The same questioning arose at the subspecies level for *O. elegans*: is there some correspondence between the diverse subspecies described and the phylogenetic clades or subclades identified? Our study as well Kyriazi et al. (2008) identified several clades and subclades on the distribution area of *O. elegans* whereas nine subspecies are currently described (Uetz et al., 2019; see Table S3 and Figure 1b). In the study of Kyriazi et al. (2008, appendix A), 34 individuals of *O. elegans* are designated by a subspecies name (*O. e. basoglui*, *O. e. blanfordi*, *O. e. centralanatoliae*, *O. e. ehrenbergii*, and *O. e. macrodactylus*). As a first approximation and pending more accurate subspecies identification (there is no precise indication in Kyriazi et al., 2008 about how the diverse subspecies have been identified), we found some correspondence between phylogroups and subspecies (see Figure S1), notably for subclade A1 (three individuals from Greece and western Turkey) and *O. e. macrodactylus* as well as for subclade A5 (eight individuals from Cyprus) and *Ophisops elegans schlueteri*. Although all samples of *O. e. basoglui* (two individuals from

south-central Turkey) and *O. e. centralanatoliae* (five individuals from eastern Turkey) are included in the same subclade A3, they nevertheless clearly constitute two distinct phylogroups (see Figure S1). On the other hand, there are no distinct phylogroups for *O. e. ehrenbergii* (11 individuals from southern Turkey and Syria) and *O. e. blanfordi* (four individuals from Syria) that are totally mixed in subclade A2. The subclade A4 could be put in correspondence with *Ophisops elegans elegans* as the type locality is located in Baku (Azerbaijan) and also because our samples from this region (Zarat) belong to this group. Concerning Iran, all *Ophisops* are supposed to belong to the subspecies *O. e. persicus* but the majority of Iranian samples are included in clade C, a result that could justify raising this subspecies to the species rank (see previous paragraph). All the Bayesian species delimitation analyses that have been conducted on *COI* clearly pointed that all genetic clusters observed would constitute separate species. However, the analyses performed on nuclear genes identified a lesser number of species as compared to the mitochondrial gene. Thus, more confident results would necessitate adding more nuclear genes for numerous individuals from all subclades (notably C1–C2 and C3–C6).

ORCID

Claudine Montgelard 🟢 https://orcid.org/0000-0002-0612-4712

REFERENCES

Agarwal, I., Khandekar, A., Ramakrishnan, U., Vyas, R., & Giri, V. B. (2018). Two new species of the *Ophisops microlepis* (Squamata: Lacertidae) complex from northwestern India with a key to Indian *Ophisops*. *Journal of Natural History*, *52*, 819–847.

Agarwal, I., & Ramakrishnan, U. (2017). A phylogeny of open-habitat lizards (Squamata: Lacertidae: Ophisops) supports the antiquity of Indian grassy biomes. *Journal of Biogeography*, *44*, 2021–2032.

Arnold, E. N., Arribas, O., & Carranza, S. (2007). Systematics of the Palaearctic and Oriental lizard tribe Lacertini (Squamata : Lacertidae : Lacertinae), with descriptions of eight new genera. *Zootaxa*, *1430*(1), 1–86. https://doi.org/10.11646/zootaxa.1430.1.1

Arnold, M. L., & Ovenden, J. R. (2010). *Le guide herpéto; 228 amphibiens et reptiles d'Europe*. Paris, France: Delachaux Et Niestlé.

Ballato, P., Mulch, A., Landgraf, A., Strecker, M. R., Dalconi, M. C., Friedrich, A., & Tabatabaei, S. H. (2010). Middle to late Miocene Middle Eastern climate from stable oxygen and carbon isotope data, southern Alborz mountains, N Iran. *Earth and Planetary Science Letters*, *300*, 125–138. https://doi.org/10.1016/j.epsl.2010.09.043

Brown, R. P., Terrasa, B., Perez-Mellado, V., Castro, J. A., Hoskisson, P. A., Picornell, A., & Ramon, M. M. (2008). Bayesian estimation of post-Messinian divergence times in Balearic Island lizards. *Molecular*

Phylogenetics and Evolution, 48, 350–358. https://doi.org/10.1016/j.ympev.2008.04.013

Darevsky, I. S., & Beutler, A. (1981). *Ophisops elegans* Menetries, 1832—Schlangenauge. In W. Bohme (Ed.), *Handbuch der Reptilien und Amphibien Europas. Band 1, Echsen (Sauria) I*. Wiesbaden (pp. 461–477). Wiesbaden, Germany: Akad. Verlagsgesellschaft.

Dayrat, B. (2005). Towards integrative taxonomy. *Biological Journal of the Linnean Society*, 85, 407–415. https://doi.org/10.1111/j.1095-8312.2005.00503.x

deMenocal, P. B. (2004). African climate change and faunal evolution during the Pliocene-Pleistocene. *Earth and Planetary Science Letters*, 220, 3–24. https://doi.org/10.1016/S0012-821X(04)00003-2

Disi, A. M. (2002). *Jordan country study on biological diversity: The herpetofauna of Jordan*. Amman, Jordan: Jordan Press Foundation.

Fortelius, M., Eronen, J., Liu, L. P., Pushkina, D., Tesakov, A., Vislobokova, I., & Zhang, Z. Q. (2006). Late Miocene and Pliocene large land mammals and climatic changes in Eurasia. *Palaeogeography Palaeoclimatology Palaeoecology*, 238, 219–227. https://doi.org/10.1016/j.palaeo.2006.03.042

Fu, J. (2000). Toward the phylogeny of the family Lacertidae - why 4708 base pairs of mtDNA sequences cannot draw the picture. *Biological Journal of the Linnean Society*, 71, 203–217.

Guo, X. G., Dai, X., Chen, D. L., Papenfuss, T. J., Ananjeva, N. B., Melnikov, D. A., & Wang, Y. Z. (2011). Phylogeny and divergence times of some racerunner lizards (Lacertidae: *Eremias*) inferred from mitochondrial 16S rRNA gene segments. *Molecular Phylogenetics and Evolution*, 61, 400–412. https://doi.org/10.1016/j.ympev.2011.06.022

Hall, T. A. (1999). BioEdit: A user-friendly biological sequence alignment editor and analysis program for Windows 95/98/NT. In *Nucleic Acids Symposium Series*, 41, 95–98.

Jorger, K. M., & Schrodl, M. (2013). How to describe a cryptic species? Practical challenges of molecular taxonomy. *Frontiers in Zoology*, 10(1), 59. https://doi.org/10.1186/1742-9994-10-59

Kapli, P., Botoni, D., Ilgaz, C., Kumlutas, Y., Avci, A., Rastegar-Pouyani, N., ... Poulakakis, N. (2013). Molecular phylogeny and historical biogeography of the Anatolian lizard Apathya (Squamata, Lacertidae). *Molecular Phylogenetics and Evolution*, 66, 992–1001.

Kapli, P., Lymberakis, P., Crochet, P.-A., Geniez, P., Brito, J. C., Almutairi, M., ... Poulakakis, N. (2015). Historical biogeography of the lacertid lizard Mesalina in North Africa and the Middle East. *Journal of Biogeography*, 42, 267–279.

Kyriazi, P., Poulakakis, N., Parmakelis, A., Crochet, P.-A., Moravec, J., Rastegar-Pouyani, N., ... Lymberakis, P. (2008). Mitochondrial DNA reveals the genealogical history of the snake-eyed lizards (*Ophisops elegans* and *O. occidentalis*) (Sauria: Lacertidae). *Molecular Phylogenetics and Evolution*, 49, 795–805. https://doi.org/10.1016/j.ympev.2008.08.021

Lanfear, R., Calcott, B., Ho, S. Y. W., & Guindon, S. (2012). PartitionFinder: Combined selection of partitioning schemes and substitution models for phylogenetic analyses. *Molecular Biology and Evolution*, 29, 1695–1701. https://doi.org/10.1093/molbev/mss020

Leigh, J. W., & Bryant, D. (2015). PopART: Full-feature software for haplotype network construction. *Methods in Ecology and Evolution*, 6, 1110–1116.

Librado, P., & Rozas, J. (2009). DnaSP v5: A software for comprehensive analysis of DNA polymorphism data. *Bioinformatics*, 25, 1451–1452. https://doi.org/10.1093/bioinformatics/btp187

Lymberakis, P., & Kaliontzopoulou, A. (2003). Additions to the herpetofauna of Syria. *Zoology in the Middle East*, 29, 33–39. https://doi.org/10.1080/09397140.2003.10637967

Maddison, W. P., & Maddison, D. R. (2018). *Mesquite: A modular system for evolutionary analysis. Version 3.51*. Retrieved from http://www.mesquiteproject.org

Matzke, N. J. (2013). BioGeoBEARS: BioGeography with Bayesian (and likelihood) evolutionary analysis in R scripts, CRAN: The Comprehensive R Archive Network, Berkeley, CA. http://CRAN.Rproject.org/package=BioGeoBEARS

Moravec, J. (1998). Taxonomic and faunistic notes on the herpetofauna of Syria (Reptilia). *Faunistische Abhandlungen des Museums fur Tierkunde Dresden*, 21, 99–106.

Oraie, H., Rahimian, H., Rastegar-Pouyani, N., Rastegar-Pouyani, E., & Khosravani, A. (2012). The easternmost record of *Ophisops elegans* (Sauria: Lacertidae) in Iran. *Herpetology Notes*, 5, 469–470.

Padial, J. M., Miralles, A., De la Riva, I., & Vences, M. (2010). The integrative future of taxonomy. *Frontiers in Zoology*, 7, 16.

Poulakakis, N., Lymberakis, P., Valakos, E., Pafilis, P., Zouros, E., & Mylonas, M. (2005). Phylogeography of Balkan wall lizard (*Podarcis taurica*) and its relatives inferred from mitochondrial DNA sequences. *Molecular Ecology*, 14, 2433–2443. https://doi.org/10.1111/j.1365-294X.2005.02588.x

Psonis, N., Antoniou, A., Karameta, E., Leache, A. D., Kotsakiozi, P., Darriba, D., ... Poulakakis, N. (2018). Resolving complex phylogeographic patterns in the Balkan Peninsula using closely related wall-lizard species as a model system. *Molecular Phylogenetics and Evolution*, 125, 100–115. https://doi.org/10.1016/j.ympev.2018.03.021

Rambaut, A., Drummond, A. J., & Suchard, M. (2013). *Tracer v1.6*. Retrieved from http://tree.bio.ed.ac.uk/software/tracer

Ronquist, F., & Huelsenbeck, J. P. (2003). MrBayes 3: Bayesian phylogenetic inference under mixed models. *Bioinformatics*, 19, 1572–1574. https://doi.org/10.1093/bioinformatics/btg180

Schlick-Steiner, B. C., Steiner, F. M., Seifert, B., Stauffer, C., Christian, E., & Crozier, R. H. (2010). Integrative taxonomy: A multisource approach to exploring biodiversity. *Annual Review of Entomology*, 55, 421–438. https://doi.org/10.1146/annurev-ento-112408-085432

Stamatakis, A. (2014). RAxML version 8: A tool for phylogenetic analysis and post-analysis of large phylogenies. *Bioinformatics*, 30, 1312–1313. https://doi.org/10.1093/bioinformatics/btu033

Struck, T. H., Feder, J. L., Bendiksby, M., Birkeland, S., Cerca, J., Gusarov, V. I., ... Dimitrov, D. (2018). Finding evolutionary processes hidden in cryptic species. *Trends in Ecology & Evolution*, 33, 153–163. https://doi.org/10.1016/j.tree.2017.11.007

Suchard, M. A., Lemey, P., Baele, G., Ayres, D. L., Drummond, A. J., & Rambaut, A. (2018). Bayesian phylogenetic and phylodynamic data integration using BEAST 1.10. *Virus Evolution*, 4, vey16. https://doi.org/10.1093/ve/vey016

Tamar, K., Carranza, S., Sindaco, R., Moravec, J., Trape, J. F., & Meiri, S. (2016). Out of Africa: Phylogeny and biogeography of the widespread genus *Acanthodactylus* (Reptilia: Lacertidae). *Molecular Phylogenetics and Evolution*, 103, 6–18. https://doi.org/10.1016/j.ympev.2016.07.003

Tamura, K., Stecher, G., Peterson, D., Filipski, A., & Kumar, S. (2013). MEGA6: Molecular evolutionary genetics analysis version 6.0. *Molecular Biology and Evolution*, 30, 2725–2729. https://doi.org/10.1093/molbev/mst197

Tang, Z. H., & Ding, Z. L. (2013). A palynological insight into the Miocene aridification in the Eurasian interior. *Palaeoworld*, 22, 77–85. https://doi.org/10.1016/j.palwor.2013.05.001

Terrasa, B., Picornell, A., Castro, J. A., & Ramon, M. M. (2004). Genetic variation within endemic *Podarcis* lizards from the Balearic Islands inferred from partial *cytochrome b* sequences. *Amphibia-Reptilia*, 25, 407–414.

Torstrom, S. M., Pangle, K. L., & Swanson, B. J. (2014). Shedding subspecies: The influence of genetics on reptile subspecies taxonomy. *Molecular Phylogenetics and Evolution*, 76, 134–143. https://doi.org/10.1016/j.ympev.2014.03.011

Uetz, P., Freed, P., & Hošek, J. (Eds.) (2019). *The reptile database*. Retrieved from http://www.reptile-database.org. Accessed september, 4th, 2019.

Venczel, M. (2006). Lizards from the late Miocene of Polgárdi (W-Hungary). *Nymphaea*, 33, 25–38.

Webb, T. III, & Bartlein, P. J. (1992). Global changes during the last 3 million years: Climatic controls and biotic responses. *Annual Reviews of*

Ecology and Systematics, *23*, 141–173. https://doi.org/10.1146/annurev.es.23.110192.001041

Yang, Z. H. (2015). The BPP program for species tree estimation and species delimitation. *Current Zoology*, *61*, 854–865. https://doi.org/10.1093/czoolo/61.5.854

Yusefi, G. H., Safi, K., & Brito, J. C. (2019). Network- and distance-based methods in bioregionalization processes at regional scale: An application to the terrestrial mammals of Iran. *Journal of Biogeography*, *46*(11), 2433–2443. https://doi.org/10.1111/jbi.13694

Zachos, F. E., Apollonio, M., Barmann, E. V., Festa-Bianchet, M., Gohlich, U., Habel, J. C., … Suchentrunk, F. (2013). Species inflation and taxonomic artefacts—A critical comment on recent trends in mammalian classification. *Mammalian Biology*, *78*, 1–6. https://doi.org/10.1016/j.mambio.2012.07.083

Zhou, Z.-S., Li, H., Tong, Q.-L., Lin, L.-H., & Ji, X. (2016). The nearly complete mitochondrial genome of the rapid racerunner *Eremias velox*, Squamata: Lacertidae. *Mitochondrial DNA*, *27*, 1781–1782.

Zuniga-Reinoso, A., & Benitez, H. A. (2015). The overrated use of the morphological cryptic species concept: An example with *Nyctelia* darkbeetles (Coleoptera: Tenebrionidae) using geometric morphometrics. *Zoologischer Anzeiger*, *255*, 47–53. https://doi.org/10.1016/j.jcz.2015.01.004

SUPPORTING INFORMATION

Additional supporting information may be found online in the Supporting Information section at the end of the article.

Figure S1. Bayesian phylogenetic tree of *COI* for 158 *Ophisops* including our 65 samples as well as 93 sequences downloaded from GenBank (Kyriazi et al., 2008). Numbers at nodes refers, from left to right, to posterior probabilities obtained with MrBayes and bootstrap proportions obtained with RaxML after 1,000 replications, respectively. Clade names are the same as defined in Kyriazi et al. (2008). The four individuals annotated by an asterisk in clade C1 represent the individuals from Kyriazi et al. (2008) whereas our six individuals falling in clade A are represented with an asterisk in clades A1 and A4 (one and five samples, respectively). The subspecies names on the right represent a tentative to link phylogroups to subspecies (see text for more details).

Figure S2. Ancestral area estimation for *Ophisops elegans* under the model DIVALIKE+j estimated with BioGeoBears. Different colors represent the seven areas defined: CY, Cyprus (pink); CZ, Central Zagros (light blue); ET, East Turkey (orange); JS, Jordan to Syria (red); NWI, North-West Iran (blue); NZ, North Zagros (green); WT, West Turkey (yellow). See Figure 1 for area delimitation.

Table S1. List of primers, reference and PCR conditions for the four genes used in this study.

Table S2. List of the datasets analyzed, number of positions and PartitionFinder results.

Table S3. List of the nine subspecies currently described for *Ophisops elegans* (Uetz, Freed & Hošek 2019; see Figure 1b).

Alignment S1. *COI* (686 positions) for 65 *Ophisops*.

Alignment S2. Concatenation (1,857 positions) of the three nuclear genes (*R35*: 690 positions, *MC1R*: 692 positions and *PKM2*: 475 positions).

APPENDIX 1

Sampling, geographic origin and NCBI accession numbers for 65 *Ophisops elegans* and three *Eremias* species (used as outgroups) as well as two *Lacerta* and four *Podarcis* species (used in the divergence dating analysis).

Taxon	Country, locality	NEZMUT or BEV collection	Cytochrome c oxidase subunit 1	R35	MC1R	PKM2
Ophisops elegans	Iran, Marakan	NEZMUT1763	MN536557			
Ophisops elegans	Iran, Marakan	NEZMUT1764	MN536558			
Ophisops elegans	Iran, Tekab	NEZMUT1765	MN536536			
Ophisops elegans	Iran, Tekab	NEZMUT1766	MN536532			
Ophisops elegans	Iran, Tekab	NEZMUT1767	MN536537			
Ophisops elegans	Iran, Tekab	NEZMUT1768	MN536533			
Ophisops elegans	Iran, Tekab	NEZMUT1769	MN536534			
Ophisops elegans	Iran, Tekab	NEZMUT1770	MN536535			
Ophisops elegans	Iran, Maku	NEZMUT1771	MN536559			
Ophisops elegans	Iran, Sahand	NEZMUT1772	MN536560			
Ophisops elegans	Iran, Sahand	NEZMUT1773	MN536561			
Ophisops elegans	Iran, Qorveh	NEZMUT1774	MN536553			
Ophisops elegans	Iran, Qorveh	NEZMUT1775	MN536554			
Ophisops elegans	Iran, Qorveh	NEZMUT1776	MN536555			
Ophisops elegans	Iran, Qorveh	NEZMUT1777	MN536556			
Ophisops elegans	Iran, Qorveh	NEZMUT1778	MN536552	MN536632	MN536609	MN536655
Ophisops elegans	Iran, Kuhrang	NEZMUT759	MN536562			
Ophisops elegans	Iran, Kuhrang	NEZMUT754	MN536563			
Ophisops elegans	Iran, Kuhrang	NEZMUT765	MN536564	MN536634	MN536611	MN536657
Ophisops elegans	Iran, Kuhrang	NEZMUT1779	MN536565			
Ophisops elegans	Iran, Kuhrang	NEZMUT1780	MN536573	MN536621	MN536598	MN536644
Ophisops elegans	Iran, Kuhrang	NEZMUT1781	MN536574			
Ophisops elegans	Iran, Shahrekord	NEZMUT1782	MN536566	MN536631	MN536608	MN536654
Ophisops elegans	Iran, Shahrekord	NEZMUT769	MN536567			
Ophisops elegans	Iran, Shahrekord	NEZMUT770	MN536568			
Ophisops elegans	Iran, Shahrekord	NEZMUT1783	MN536569	MN536622	MN536599	MN536645
Ophisops elegans	Iran, Amrulah	NEZMUT1784	MN536570	MN536630	MN536607	MN536653
Ophisops elegans	Iran, Amrulah	NEZMUT1785	MN536571			
Ophisops elegans	Iran, Amrulah	NEZMUT1786	MN536572			
Ophisops elegans	Iran, Sarab	NEZMUT1787	MN536575	MN536629	MN536606	MN536652
Ophisops elegans	Iran, Sarab	NEZMUT1788	MN536576	MN536625	MN536602	MN536648
Ophisops elegans	Iran, Oshtorankuh	NEZMUT1789	MN536577	MN536628	MN536605	MN536651
Ophisops elegans	Iran, Oshtorankuh	NEZMUT1790	MN536578	MN536623	MN536600	MN536646
Ophisops elegans	Iran, Oshtorankuh	NEZMUT1791	MN536579			
Ophisops elegans	Iran, Oshtorankuh	NEZMUT1792	MN536580			
Ophisops elegans	Iran, Bukan	NEZMUT1793	MN536581			
Ophisops elegans	Iran, Bukan	NEZMUT1794	MN536582			
Ophisops elegans	Iran, Bukan	NEZMUT1795	MN536583	MN536624	MN536601	MN536647
Ophisops elegans	Iran, Alvand	NEZMUT1796	MN536539			
Ophisops elegans	Iran, Alvand	NEZMUT1797	MN536540			
Ophisops elegans	Iran, Alvand	NEZMUT1798	MN536541			
Ophisops elegans	Iran, Alvand	NEZMUT1799	MN536542			
Ophisops elegans	Iran, Alvand	NEZMUT1800	MN536538			

(Continues)

APPENDIX 1 (Continued)

Taxon	Country, locality	NEZMUT or BEV collection	Cytochrome c oxidase subunit 1	R35	MC1R	PKM2
Ophisops elegans	Iran, Zanjan	NEZMUT1801	MN536584			
Ophisops elegans	Iran, Zanjan	NEZMUT1802	MN536585			
Ophisops elegans	Iran, Zanjan	NEZMUT1803	MN536586	MN536635	MN536612	MN536658
Ophisops elegans	Iran, Sarpol	NEZMUT1804	MN536587	MN536636	MN536613	MN536659
Ophisops elegans	Iran, Sarpol	NEZMUT1805	MN536588			
Ophisops elegans	Iran, Sarpol	NEZMUT1806	MN536589	MN536620	MN536597	MN536643
Ophisops elegans	Iran, Aleshtar	NEZMUT1807	MN536590			
Ophisops elegans	Iran, Aleshtar	NEZMUT1808	MN536591	MN536637	MN536614	MN536660
Ophisops elegans	Iran, Shazand	NEZMUT1809	MN536592	MN536626	MN536603	MN536649
Ophisops elegans	Iran, Shazand	NEZMUT1810	MN536593			
Ophisops elegans	Iran, Shazand	NEZMUT1811	MN536594	MN536638	MN536615	MN536661
Ophisops elegans	Iran, Avaj	NEZMUT1812	MN536595			
Ophisops elegans	Iran, Avaj	NEZMUT1813	MN536596	MN536639	MN536616	MN536662
Ophisops elegans	Azerbaidjan, Zarat	BEV11689	MN536544	MN536633	MN536610	MN536656
Ophisops elegans	Azerbaidjan, Zarat	BEV11690	MN536545			
Ophisops elegans	Azerbaidjan, Zarat	BEV11691	MN536546			
Ophisops elegans	Azerbaidjan, Lerik	BEV11712	MN536547			
Ophisops elegans	Azerbaidjan, Lerik	BEV11713	MN536548			
Ophisops elegans	Azerbaidjan, Lerik	BEV11714	MN536549			
Ophisops elegans	Azerbaidjan, Lerik	BEV11715	MN536550			
Ophisops elegans	Azerbaidjan, Lerik	BEV11716	MN536551			
Ophisops elegans	Turkey, Akseki	BEV11022	MN536543	MN536627	MN536604	MN536650
Eremias velox	Azerbaidjan, Zarat	BEV11692	KM359148[a]	MN536640	MN536617	MN536663
Eremias arguta	Azerbaidjan, Salyan	BEV11719	HQ733920[b]	MN536642	MN536619	MN536665
Eremias persica	Iran, Khoshyeylagh	RBTG006	HQ733941[c]	MN536641	MN536618	MN536664
Podarcis lilfordi			KF003303[d]			
Podarcis pityusensis			KF003304[c]			
Podarcis cretensis			KF003298[c]			
Podarcis peloponnesiacus			KF003299[c]			
Lacerta agilis			KP697866[d]			
Lacerta viridis			KP697870[d]			

Note: All sequences were produced in this study to the following exceptions: [a]Zhou, Li, Tong, Lin, and Ji (2016); [b]Guo, X., Chen, D., Papenfuss, T. J. and Wang, Y., unpublished; [c]Kapli et al. (2013); [d]Hawlitschek, O., Dunz, A., Franzen, M., Jerome, M., Roedder, D., Glaw,F. and Haszprunar, G., unpublished.

Abbreviations: BEV: Biogéographie et Ecologie des Vertébrés (Centre d'Ecologie Fonctionnelle et Evolutive, Montpellier, France); NEZMUT: Natural Environment, Zoological Museum (University of Tehran, Iran).